

Texture Evolution of a 2.8 wt% Si Non-Oriented Electrical Steel during Hot Band Annealing

Mehdi Mehdi^{1,2}, Youliang He^{1*}, Erik J. Hilinski³, Afsaneh Edrissy²

¹CanmetMATERIALS, Natural Resources Canada, Hamilton, ON, Canada L8P 0A5

²Department of Mechanical, Automotive, and Materials Engineering, University of Windsor, Windsor, ON, Canada N9B 3P4

³Tempel Steel Co., Chicago, IL, USA 60640-1020

*Corresponding author: youliang.he@canada.ca

Abstract. To optimize the magnetic properties of non-oriented electrical steels, it is necessary to carefully control all the stages of thermomechanical processing during the production of the steel sheets, since the microstructure and crystallographic texture at an early step will usually affect those at the subsequent steps. Many studies have shown that hot band annealing may have a positive effect on the texture of the final sheet, but it is not clear what are the optimal annealing conditions to obtain the desired final textures. In this study, the evolution of microtexture and microstructure of a 2.8 wt% Si non-oriented electrical steel during hot band annealing is studied by using electron backscatter diffraction (EBSD) techniques. A region of the hot-rolled sample was marked by micro-indents so that the same area could be examined at various annealing times (under the same temperature) to investigate the evolution of the microstructure and microtexture during recrystallization. In this way, the mechanisms of texture evolution was elucidated, and optimal annealing conditions can be determined.

1. Introduction

Electrical steel is a soft magnetic material that is commonly used in transformers, motors, generators, alternators, etc. [1-6]. Superior magnetic properties are thus needed for such applications which involve decreasing hysteresis and eddy current losses in addition to increasing permeability [2]. The magnetic properties of electrical steel are dependent on many factors including silicon content, grain size, sheet thickness, residual stress as well as crystallographic texture. It is well known that the magnetic properties of electrical steel are orientation dependent due to the fact that the easy magnetization directions are along the $\langle 001 \rangle$ axes and the hard magnetization directions are along the $\langle 111 \rangle$ axes [2-6]. Therefore, to improve the magnetic properties of electrical steel, the $\langle 001 \rangle$ //ND (θ -fibre) texture (ND is the normal direction) should be enhanced which includes both the cube $\{001\}\langle 010 \rangle$ and rotated cube $\{001\}\langle 110 \rangle$ orientations, while the $\langle 111 \rangle$ //ND (γ -fibre) texture must be suppressed in the final sheet [3, 4].



The final texture of electrical steel is highly dependent on the manufacturing process. The texture evolves during solidification, plastic deformation, dynamic recrystallization, phase transformation, static recrystallization and grain growth [3]. During cold rolling of non-oriented electrical steel, a strong γ -fibre $\langle 111 \rangle // \text{ND}$ and an α -fibre $\langle 110 \rangle // \text{RD}$ (RD is the rolling direction) usually develop especially around the $\{001\} \langle 110 \rangle$ and $\{112\} \langle 110 \rangle$ orientations. After annealing there is a significant decrease in the α -fibre and an increase in the $\{111\} \langle 112 \rangle$ component (on the γ -fibre). The observed textures after annealing are generally related to the deformation texture with an orientation of 20-30° rotation about the $\langle 110 \rangle$ and $\langle 100 \rangle$ axes [7]. Several unconventional methods have been examined in the literature to optimize the texture of electrical steels which included columnar grain growth, cross rolling, two stage cold rolling, inclined and skew rolling [3, 5-6].

In the literature, several studies have examined the effect of the hot rolling texture on the final texture developed after cold rolling and final annealing [8-12]. Some of them found that the increase in grain size of the hot band played a significant role in increasing the magnetic permeability of electrical steel while simultaneously decreasing the core losses [9, 10]. Others observed a correlation between the formation of shear band and micro-band and the recrystallization of magnetically favorable crystal orientations (e.g. Goss and Cube), which decreases the volume fraction of the magnetically detrimental $\langle 111 \rangle // \text{ND}$ orientations. On the other hand, some studies [8] have shown that annealing after hot rolling has no effect or has a negative effect on the magnetic properties of the final sheet after cold rolling and annealing. Thus, it is important to understand the texture formation during hot rolling and the subsequent annealing to be able to make understand the texture evolution after cold rolling and final annealing. In this paper the texture evolution was tracked after hot rolling and annealing at the same area up to 160 minutes at 800 °C. Correlations were observed between the initial texture formed during hot rolling and the annealing texture at several different regions of the hot-rolled electrical steel plate.

2. Experimental

The chemical composition of (wt%) of the electrical steel used in this study is: 2.77 Si, 0.52 Al, 0.3 Mn, 0.01 P, and 0.003 C. It was melted in a vacuum furnace and cast into ingots with a cross-sectional area of $200 \times 200 \text{ mm}^2$. It was then heated up to a nominal temperature of 1038 °C and hot rolled to a thickness of 25 mm in six passes with ~87.5% reduction. The surface oxides were then machined before the second hot rolling process. The steel plates were heated up to 1038 °C again and hot rolled in six passes down to a final thickness of ~3.5 mm (~85% reduction). The plates were finally pickled in a HCl solution to remove surface oxides generated during the second hot rolling.

One hot-rolled plate was cut into a small rectangular piece which was then prepared using conventional metallographic procedures for EBSD characterization. To track the same region throughout the entire study, a rectangular area in the ND-RD plane was marked with several indentations that could be readily located during the SEM analysis. EBSD characterizations were performed in a field emission gun SEM (Nova NanoSEM, FEI) which is equipped with an EDAX Orientation Imaging Microscopy system (OIM 6.2). The scans covered the entire thickness of the plate. Orientation distribution functions (ODFs) were calculated using harmonic series expansion method with a Gaussian half-width of 5° and a series rank of 22. Texture components were plotted on the $\varphi_2 = 45^\circ$ section of the Euler space (Bunge notation).

The sample was then annealed at 800 °C for various times in argon protected atmosphere and subsequently water quenched to freeze the microstructures. The furnace was first raised to the desired temperature and the sample was inserted into a region inside the furnace that had a uniform temperature distribution. Following each annealing process, an EBSD scan was conducted at the exact same location that was marked with indentations. A very slight polishing step was applied using a colloidal silica solution after each annealing experiment.

3. Results and Discussion

The microstructure and texture of the hot-rolled plate is shown in Figure 1, which showed apparent heterogeneity across the thickness of the sample. The microstructure can be divided into three regions, i.e. A, B and C. Region A starts from the surface and extends about 800 μm towards the center. This region is composed of both deformed coarse grains at the surface and dynamically recrystallized fine grains beneath them. The dominant textures (Figure 2a) in region A include Copper $\{112\} \langle 111 \rangle$, Goss $\{110\} \langle 001 \rangle$ and Brass $\{110\} \langle 112 \rangle$. These textures are often observed in cold rolled fcc metals such as Al, Ni, Cu and Ag [7]. Region B is immediately below Region A and extends $\sim 250 \mu\text{m}$ towards the center. This region is composed of several elongated grains with $\langle 011 \rangle // \text{ND}$ orientations (green) and some other smaller grains embedded between them. The texture (Figure 2b) is essentially a single orientation at $\{110\} \langle 001 \rangle$ (the Goss texture). Region C is at the middle of the rolled plate and spreads about 1/3 of the thickness. The microstructure is composed of several elongated grains with different orientations (different colors). Some of these grains have very large ingrain misorientations ($>10^\circ$), e.g. left side of Region C. The texture (Figure 2c) of this region mainly consists of an α -fibre ($\langle 110 \rangle // \text{RD}$) and a γ -fibre ($\langle 111 \rangle // \text{ND}$), and the strongest orientation is the rotated cube $\{001\} \langle 110 \rangle$. This texture is very similar to the typical cold-rolling texture of bcc metals [1,7].

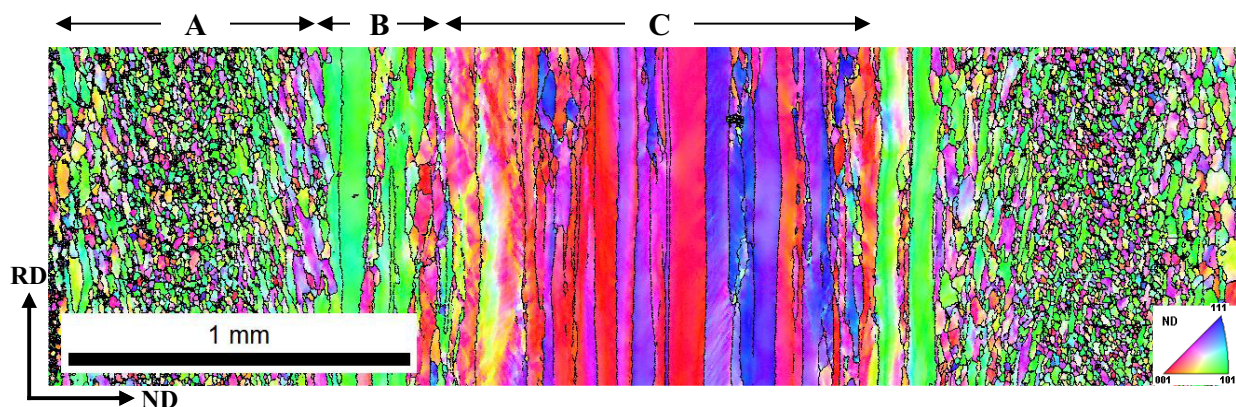


Figure 1. EBSD inverse pole figure (IPF) map of a hot-rolled 2.8% Si steel on the ND-RD plane showing the three different regions A, B and C.

The near surface textures (regions A and B) are developed due to the strong shear stress between the rolls and the surfaces of the material. This shear stress is the result of friction and is parallel to the rolling direction, which will rotate the crystal around the transverse direction (TD). In fact, a simple 90° -rotation of the texture at the center region (Region C) around the TD will give rise to a texture very similar to what was observed in Region A. Holscher et al. [13] explained the relationship between the rolling textures and the shear textures in bcc metals as a result of slip symmetry, which arises from the slip system with a 0 Schmidt factor turning into a maximum Schmidt factor system when a rotation of the lattice occurs by 45° . The overall texture of the material in the ND-RD plane (including all regions) is shown in Figure 2d, which shows a strong rotated cube, an α -fibre, a Goss component and some other orientations.

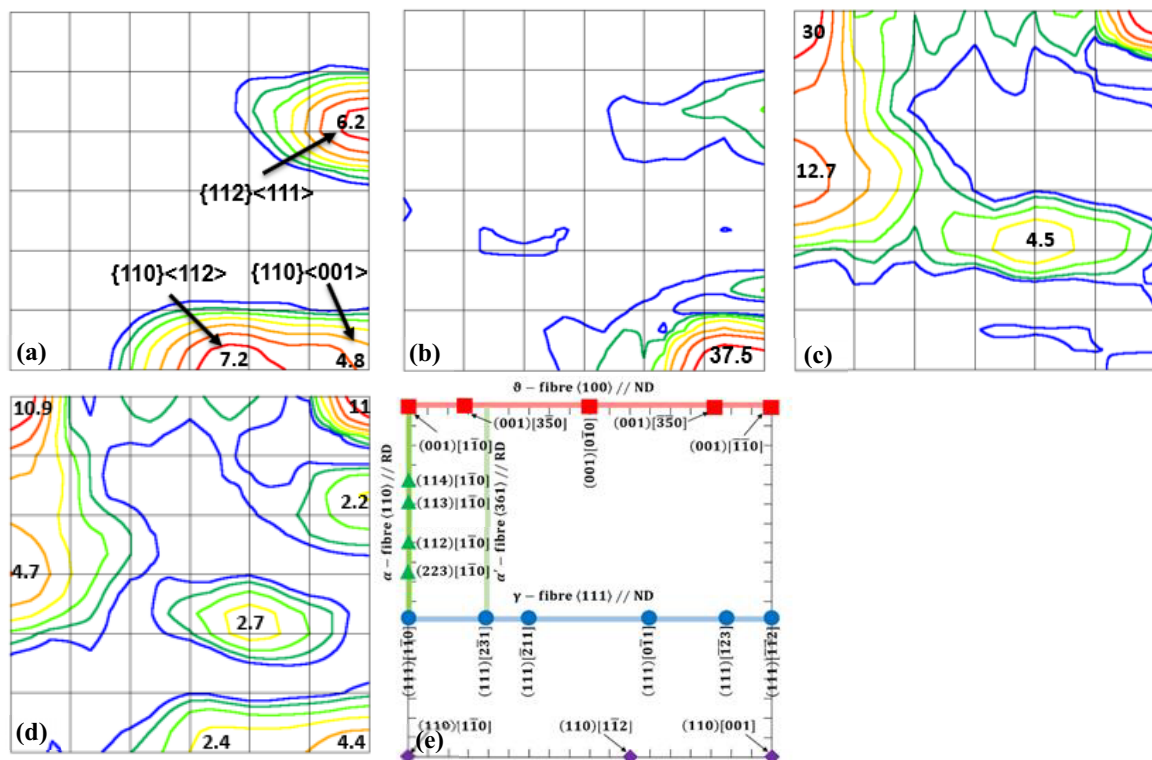


Figure 2. $\varphi_2 = 45^\circ$ sections of the ODF for different regions of the hot-rolled plate: (a) Region A, (b) Region B, (c) Region C, (d) overall including all regions, and (e) texture key.

The evolution of texture in the surface regions (Regions A and B) during annealing is shown in Figure 3. As the annealing time increases, the overall texture intensity generally decreases. The Goss texture apparently decreases with the annealing time, while the copper ($\{112\}\langle 111\rangle$) and brass ($\{110\}\langle 112\rangle$) components essentially do not change until the annealing time increases to 110 minutes. After 160 minutes, all the components are significantly weakened. The copper and brass orientations have a higher Taylor factor than the Goss orientation, thus having more stored energy than Goss, which caused them to recrystallize first. During recrystallization, new copper and brass crystals nucleate from the originally deformed copper and brass crystals, and they grow into the deformed Goss matrix and consume the Goss grains. This is due to the fact that the misorientation relationship between the deformed Goss and the copper and brass orientations is all within $25\text{-}35^\circ\langle 110\rangle$, which is very close to high mobility CSL boundaries, i.e. $\Sigma 19a$ ($26.5^\circ\langle 110\rangle$) and $\Sigma 9$ ($38.9^\circ\langle 110\rangle$).

As the annealing time increases to more than 30 minutes, new orientations, e.g. $\{111\}\langle 148\rangle$, start to appear (Figure 3b). This orientation is close to the stable bcc recrystallization $\{111\}\langle 011\rangle$ orientation. It becomes more prominent and stable with the increase of annealing time (Figure 3c). A $\{443\}\langle 338\rangle$ orientation also starts to appear after 110 minutes, which is very close to the two stable deformation orientations $\{111\}\langle 112\rangle$ and $\{441\}\langle 118\rangle$. These latter orientations usually form from plane-strain deformation of the $\{110\}\langle 001\rangle$ orientation [11]. After 60 minutes (Figure 3c), a $\{555\}\langle 135\rangle$ orientation starts to appear and it becomes stronger with the increase of annealing time (Figures 3d and 3e). After 160 minutes, the original shearing textures change to final components such as $\{110\}\langle 112\rangle$, $\{555\}\langle 135\rangle$, $\{443\}\langle 338\rangle$ and $\{110\}\langle 118\rangle$.

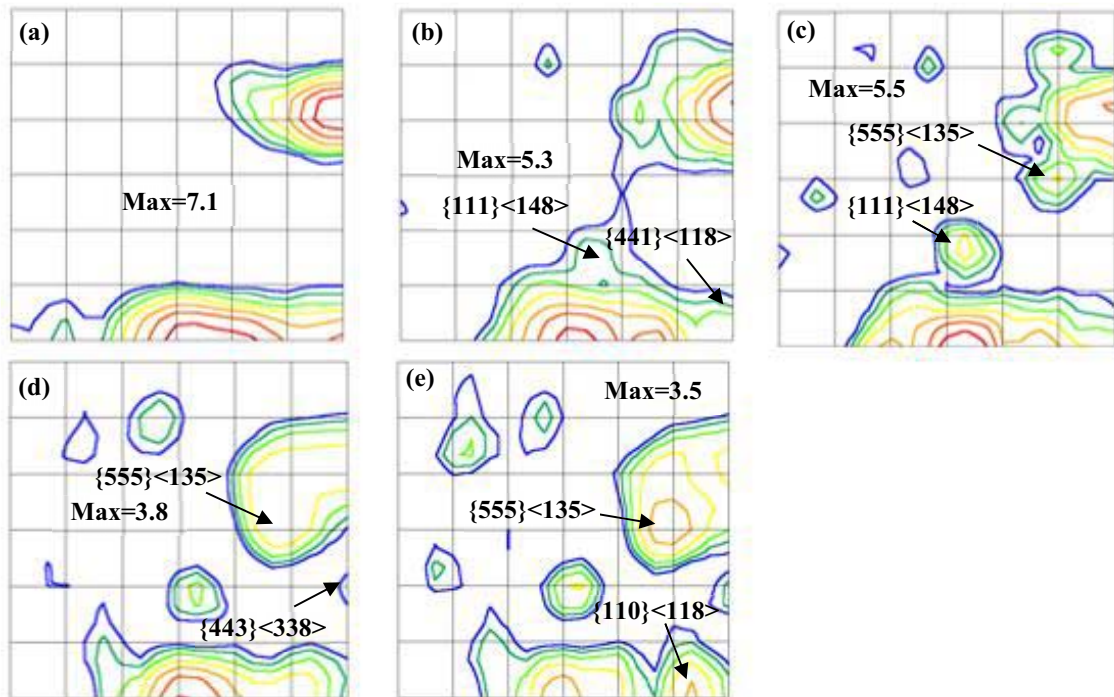


Figure 3. $\varphi_2 = 45^\circ$ sections of the ODF after annealing at 800 °C for various times (Regions A and B): (a) as hot rolled (0 minutes), (b) 30 minutes, (c) 60 minutes, (d) 110 minutes, and (e) 160 minutes.

The evolution of texture in the middle region of the hot band (Region C) is shown in Figure 4. Recrystallization starts at the deformed γ -fibre grains (either at shear bands, microbands or grain boundaries) and they are the first to be consumed as seen from the decrease of their intensity from Figure 4a to Figure 4b. Again it is due to the high Taylor factor and high stored energy of these grains. As the annealing time increases to 60 minutes (Figure 4c), a $\{113\}\langle 361\rangle$ orientation starts to appear which is on the α^* -fibre ($\{11h\}\langle 12\frac{1}{h}\rangle$). This fibre becomes strong and prominent when the annealing time is increased to 110 minutes (Figure 4d). The α -fibre generally weakens with the increase of annealing time, and the only exception is that the $\{111\}\langle 110\rangle$ component (which belongs to both the α - and γ -fibres) first weakens with time and then strengthens again after 110 minutes. The rotated cube orientation remains stable and strong until 110 minutes. Beyond that, it weakens significantly with the formation a $\{001\}\langle 350\rangle$ component. A $\{118\}\langle 081\rangle$ component also starts to form when the annealing time is 30 minutes, and it strengthens with the increase of the annealing time.

An interesting feature to be noticed in this region (Region C) is the strengthening of the Goss orientation with annealing time. It should be noted that this orientation was not present in the central region in the deformed state as it was not stable under plane-strain deformation. Several studies [9, 14] have found that the Goss is only present in the shear bands and microbands of the $\{111\}\langle 112\rangle$, $\{111\}\langle 110\rangle$ or $\{112\}\langle 110\rangle$ deformed grains. During hot rolling, no shear bands were noticed in these grains in Region C. Thus, the nucleation and growth of the $\{110\}\langle 001\rangle$ orientations cannot be attributed to the same mechanism that gives rise to this orientation after cold rolling and primary recrystallization.

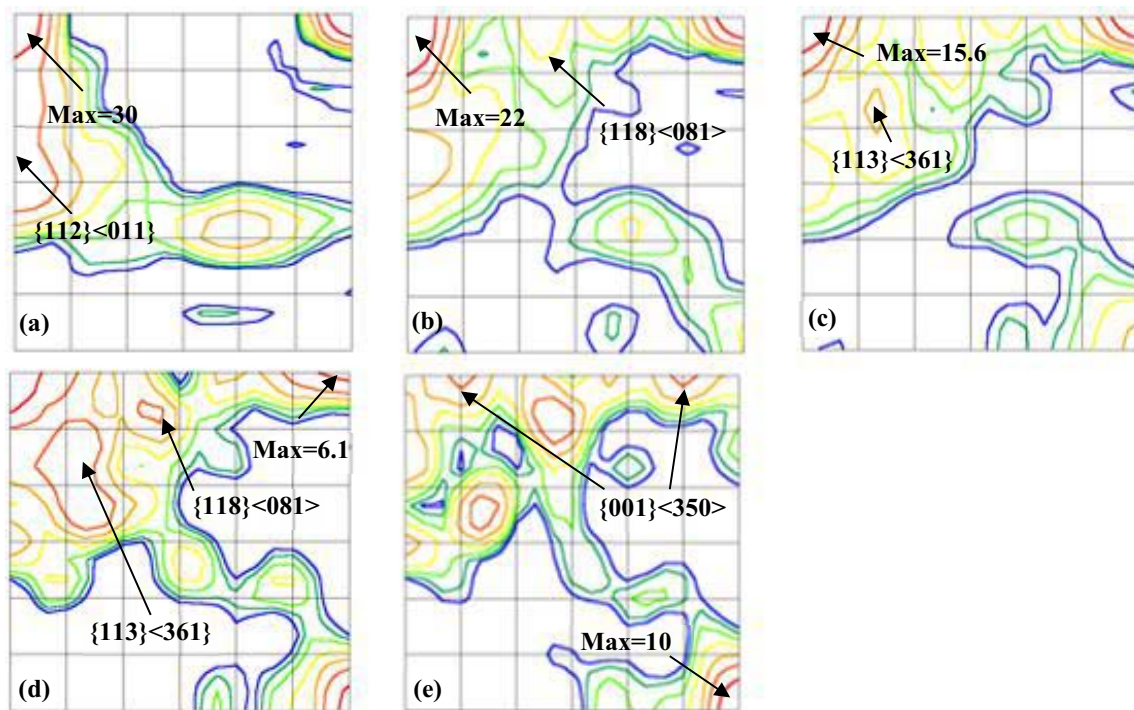


Figure 4. $\varphi_2 = 45^\circ$ sections of the ODF showing the evolution of texture (Region C) during annealing at 800 °C for various times: (a) as hot rolled (0 minutes), (b) 30 minutes, (c) 60 minutes, (d) 110 minutes, and (e) 160 minutes.

The microstructure during and after hot rolling is very complicated due to the fact that several processes occur simultaneously, e.g. plastic deformation, dynamic recovery and recrystallization, static recovery and recrystallization. In an attempt to understand the reason for the formation of a large shear-textured zone in the microstructure, the following mechanism is proposed. The shear stress generated during hot rolling cannot be large enough to influence the grains ~ 1.2 mm below the surface. Thus, a thinner shear deformation zone is believed to be generated during the first hot rolling process (when the thickness was reduced from 200 mm to 25 mm). The consequent annealing at a temperature of 1038 °C allowed the surface textures to grow well below the surface of the hot-rolled plate. This growth of the shearing textures can be attributed to two factors: (a) the high strain and elevated temperature that are present near the surface allow the region to recrystallize and grow before the central region; the recrystallized grains grow and consume the inner deformed matrix and thus extending the shear-textured region; (b) the Goss orientation which forms at the bottom of the shear-textured zone (corresponding to Region B in Figure 1) is well known to have a faster mobility than other orientations, which is due to the fact that the Goss $\{110\}\langle 001\rangle$ possess a high angle grain boundary with respect to the major texture components (copper and brass) in the deformed region above it and below it (α -fibre and γ -fibre). The brass and copper orientations both have a misorientation angle of $\sim 35^\circ$ about the $\langle 110\rangle$ axis to the Goss orientation. This misorientation has been quoted in several studies [1, 9] to have a high angle mobility in comparison with other misorientations. A schematic summary of the suggested mechanism is shown in Figure 5a. A similar mechanism was observed in the evolution of the texture in Region C. The Goss intensity increased with annealing time despite the absence of any observable shear bands in the central region. This once again could be explained as the Goss orientation growing into the deformed regions rather than nucleating therein.

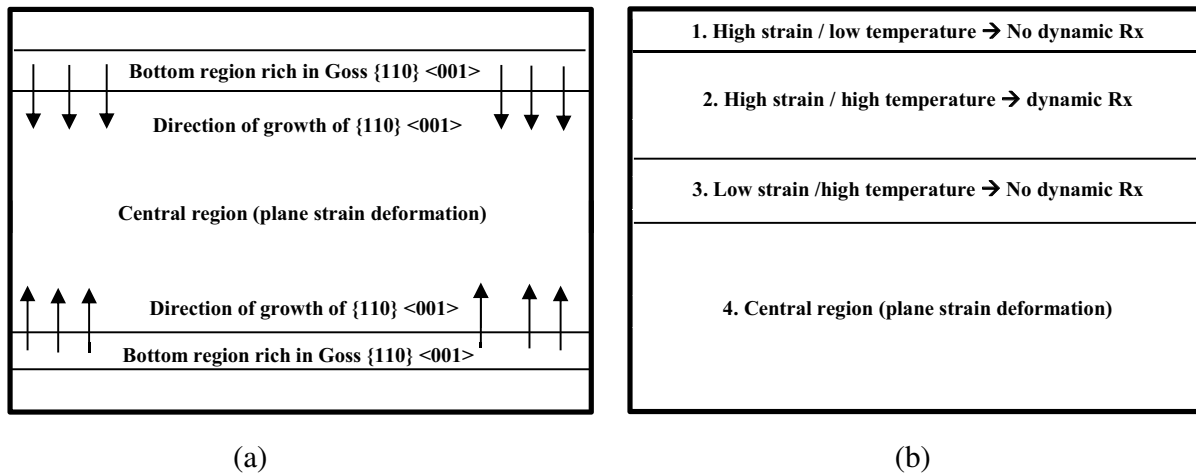


Figure 5. The proposed mechanism for the formation of texture and microstructure during hot rolling of electrical steel: (a) the growth of the Goss grains into the deformed central region after the first hot rolling process, (b) the difference in microstructure and texture in the upper 1/3 of the plate due to variation in strain and temperature.

Another interesting feature in the hot-rolled electrical steel is the existence of multiple dissimilar regions in the upper 1/3 of the hot-rolled plate. A schematic representation of the several inhomogeneous layers is shown in Figure 5b. The differences in microstructure and texture among these regions can be explained as follows: the upper surface region (Region 1 in Figure 5b) is composed of long elongated grains without fine grains embedded in the microstructure. This is due to the fact that despite the strain being extremely high in this region, the direct contact of the surfaces with the rolls decreases the surface temperature and thus does not allow dynamic or static recrystallization to occur. The central region of the top 1/3 of the plate (Region 2 in Figure 5b) is very close to the surface, thus the shear strain is high. On the other hand, the temperature in this inner region is high enough (not in contact with the rolls), which combines with the high strain to result in dynamic and static recrystallization (the fine grains shown in Region A in Figure 1). The bottom region of the upper 1/3 of the hot-rolled plate (Region 3 in Figure 5b) is far away from the surface and thus has a low strain but a high temperature. These combined conditions prevent the occurrence of recrystallization. Finally the central region of the hot-rolled plate is far away from the rolls, thus the shear strain is negligible, which results in the typical bcc rolling texture and microstructure.

4. Summary

The microstructure and texture across the thickness of hot-rolled electrical steel plate are significantly different due to the differences in deformation mode (i.e. shear or plane strain) and temperature.

For dynamic or static recrystallization to occur at the surfaces, both high shear-strain and high temperature should be present. These two conditions are only present in regions immediately below the surfaces, thus recrystallized microstructure and texture exist in these regions.

The center region of the plate is not subjected to shear deformation, therefore it does not recrystallize during hot rolling, which results in the typical bcc rolling microstructure and texture.

During annealing, the intensity of the $\{110\}\langle 001 \rangle$ decreases in the surface layer (Region A) and increases in central region (Region C) with annealing time.

Acknowledgements

The Program of Energy Research and Development, Natural Resources Canada, and the Natural Sciences and Engineering Research Council of Canada are gratefully acknowledged for financial support. Renata Zavadil and Jian Li are thanked for their help on the EBSD measurements.

References

1. Humphreys, F. J., & Hatherly, M. (2012). Recrystallization and related annealing phenomena. Elsevier.
2. Mehdi, M., He, Y., Hilinski, E. J., & Edrissy, A. (2017). Effect of skin pass rolling reduction rate on the texture evolution of a non-oriented electrical steel after inclined cold rolling. *Journal of Magnetism and Magnetic Materials*, 429, 148-160.
3. Kestens, L., & Jacobs, S. (2008). Texture control during the manufacturing of nonoriented electrical steels. *Texture, Stress, and Microstructure*, 2008.
4. Rollett, A. D., Storch, M. L., Hilinski, E. J., & Goodman, S. R. (2001). Approach to saturation in textured soft magnetic materials. *Metallurgical and Materials Transactions A*, 32(10), 2595-2603.
5. He, Y., & Hilinski, E. J. (2017). Skew rolling and its effect on the deformation textures of non-oriented electrical steels. *Journal of Materials Processing Technology*, 242, 182-195.
6. He, Y., Hilinski, E., & Li, J. (2015). Texture evolution of a non-oriented electrical steel cold rolled at directions different from the hot rolling direction. *Metallurgical and Materials Transactions A*, 46(11), 5350-5365.
7. Hu, H. (1974). Texture of metals. *Texture, Stress, and Microstructure*, 1(4), 233-258.
8. Pedrosa, J. S. M., da Costa Paolinelli, S., & Cota, A. B. (2015). Influence of initial annealing on structure evolution and magnetic properties of 3.4% Si non-oriented steel during final annealing. *Journal of Magnetism and Magnetic Materials*, 393, 146-150.
9. Park, J. T., & Szpunar, J. A. (2009). Effect of initial grain size on texture evolution and magnetic properties in nonoriented electrical steels. *Journal of Magnetism and Magnetic Materials*, 321(13), 1928-1932.
10. R. Takanohashi, F.J.G. Landgraf, Effect of hot-band grain size and intermediate annealing on magnetic properties and texture of non-oriented silicon steels, *J. Magn. Magn. Mater.* 304 (2006) 608–610.
11. T. Haratani, W.B. Hutchinson, I.L. Dillamore, P. Bate, Contribution of shear banding to origin of Goss texture in silicon steel, *Met. Sci.* 18 (1984) 57–65.
12. S.C. Paolinelli, M.A. Cunha, A.B. Cota, The influence of shear bands on final structure and magnetic properties of 3% Si non-oriented silicon steel, *J. Magn. Magn. Mater.* 320 (2008) 641–644.
13. Hölscher, M., Raabe, D., & Lücke, K. (1994). Relationship between rolling textures and shear textures in fcc and bcc metals. *Acta metallurgica et materialia*, 42(3), 879-886.
14. Dorner, D., Zaefferer, S., & Raabe, D. (2007). Retention of the Goss orientation between microbands during cold rolling of an Fe3% Si single crystal. *Acta materialia*, 55(7), 2519-2530.